

Gate-Induced Drain Leakage: A Brief Survey on Effects Applications and modeling

¹B. Balaji Naik , ²Srinivasa Rao Thamanam, ³Srinivas Sabbavarapu⁴K. Manjunathachari

¹Assistant Professor, School of Technology, GITAM (Deemed to be University), Hyderabad, Telangana, India.

²Assistant Professor, School of Technology, GITAM (Deemed to be University), Hyderabad, Telangana, India.

³Associate Professor, Anil Neerukonda Institute of Technology and Sciences(UGC Autonomous), Visakhapatnam, A.P, India

⁴ Professor, School of Technology, GITAM (Deemed to be University), Hyderabad, Telangana, India
¹bbukke@gitam.edu, ²sthamana@gitam.edu, ³ssrinivas.ece@anits.edu.in, ⁴mkamsali@gitam.edu

Article Info

Volume 83

Page Number: 2303 - 2315

Publication Issue:

May - June 2020

Abstract:

The advent of Internet Of Things (IOT) made the remote healthcare a promising Scaled oxide thickness plays a vital role in sub-micron (<20nm) technology nodes where leakage currents contributes its major share. In quest of low power designs, Gate-Induced Drain Leakage (GIDL) draws great attention, which is an important phenomenon at drain gate overlap. The GIDL is the major of all leakage currents sources in a transistor which influences the operation of Dynamic Random Access Memory (DRAM). DRAM's performance, in terms of retention time, is greatly influenced by OFF-STATE leakage in MOSFET. The DRAM cell size reduction, usually employs gate oxide thickness reduction to minimize short-channel effects, including sub-threshold leakage, while maximizing trans-conductance and saturation current. As adverse effect, the electric field developed underneath the gate increases by reducing gate oxide thickness, making the transistor more susceptible to GIDL. Further, Band-To-Band Tunneling (BTBT) increases the GIDL of MOSFET, and generation of interface traps causes Trap-Assisted Two-Step Tunneling (TATT) to increase the GIDL. In this article, a brief survey of different modeling methods for GIDL along with its effects and applications has been presented.

Keywords: Digital Watermarking, Medical Imaging, MIPAS (medical image processing and. archiving system), Hospital Information Systems (HIS)

Article History

Article Received: 11August 2019

Revised: 18November 2019

Accepted: 23January 2020

Publication: 10May2020

I. Introduction

The performance of a FET at submicron technology, greatly affected by the leakage currents in off state of a transistor which makes the output to change with time. Among all the leakage phenomena's Gate-induced drain leakage current (GIDL) occupies the major share [1]. To minimize the current (leakage) during off state of a transistor, it is essential to work on reduction of this GIDL by understanding the causes of it in low-power integrated circuits. As the gate induces high field, near the overlap region of drain-gate(deep-depleted), band-to-band tunneling

(BTBT) process at Si/SiO₂ interface is attributed by GIDL [1]. MOSFET leakage current shows its clear impact in retention time degradation, during the off state of a transistor DRAM's. Generally, the off-state leakage is observed due to electron hole pairs generated at the junction (in space charge region), sub-threshold channel leakage, punch-through and GIDL. The GIDL (drain to channel leakage), varies with the gate bias because of its dependency on the junction electrical field. As it is essential to reduce the DRAM cell size for better integration, usually the gate oxide thickness is targeted for the with a minimization of adverse effects of short-

channel, sub-threshold leakage and their side effects while maximizing trans-conductance and operational current (saturation). The electric field under the gate increases transistor susceptibility to GIDL, with reduced gate oxide thickness. Furthermore, the induction of hot-carrier spurred great research interest among the research community, in deep submicron domain, for the reliability of transistor and thereby circuit [2]. After stress, the GIDL, threshold voltage (V_{th}), trans-conductance (g_m), drain current (I_d) and oscillator frequency have a great role to play in the degradation of hot carriers.

In this paper, an effort was made to enlighten different effects and applications of GIDL in scaled FETs and different modeling methods. In the remainder of the article: section II narrates the impact of GIDL and the different elements and processes that effect GIDL. Different architectures and their application in GIDL were discussed in section III, section IV looks into different modeling's for GIDL and its analysis and with conclusions in section V.

II. Effects On GIDL Current And Its Impact

The supply voltage, power and gate oxide are anticipated to be intensively scaled down with scaling of MOSFET technology to the sub-half-micron region, inducing a decent and significant GIDL [3]. A study of GIDL current degradation in lightly-doped drain (LDD) nMOSFETs is presented in [3]. The degradation is analyzed and different methods for degradations were decoupled (using stress pulse) with different parameters (combination) like amplitude, frequency, rise time, fall time and major effects of hot-carriers (with maximum substrate and gate currents). LDD nMOSFETs use 0.35 μm CMOS technology. HP4156B analyzer for semiconductor parameters is used, with channel length of 0.35 μm and width 10 μm , respectively. for characterizing and performing stress experiments. The GIDL characteristics were measured, pre and post-stress, with gate bias V and grounded substrate and source. As shown in Fig. 1, channel to drain (sub-

threshold/diffusion) leakage, causes the leakage in drain to increase.

The impact of GIDL on the sub micrometer leakage is studied in [5]. GIDL, with regards to off-state current, constitutes a serious constraint.

Vertical MOSFETs have non-identical source and drains, unlike the conventional ones. The drain leakage currents are investigated in [5] due to asymmetric drain and source geometries of vertical MOSFET's surround-gate. Configurations like drain-on-bottom and drain-on-top were used for measurements of GIDL and body leakage, as a function of temperature, in a transistor. On interchange of drain and source terminals, asymmetric leakage currents were observed with higher body leakage in the drain-on-top and higher GIDL in drain-on-bottom. From measurements, in the temperature ranges of $-50 - 200^\circ\text{C}$, the asymmetric body leakage differed with use of ap-well ion implantation. This asymmetric is due to the variation SiO₂ thickness (at gate) on horizontal $\langle 100 \rangle$ wafer surface and the vertical $\langle 110 \rangle$ pillars sidewalls. The origin of this asymmetry is investigated through simulations, with the help of a simplified model using the gated diodes, (Fig. 2).

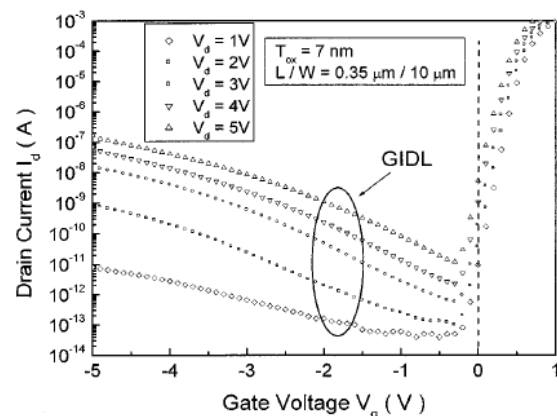


Fig. 1. Measurement of GIDL with variation in drain bias [3].

The simulations were done for the doping profile using SIMS doping profiles which are measured calibrated to values of sheet resistance. For simplicity, the constant body doping profile was considered for the structure body, as it has negligible effect on GIDL.

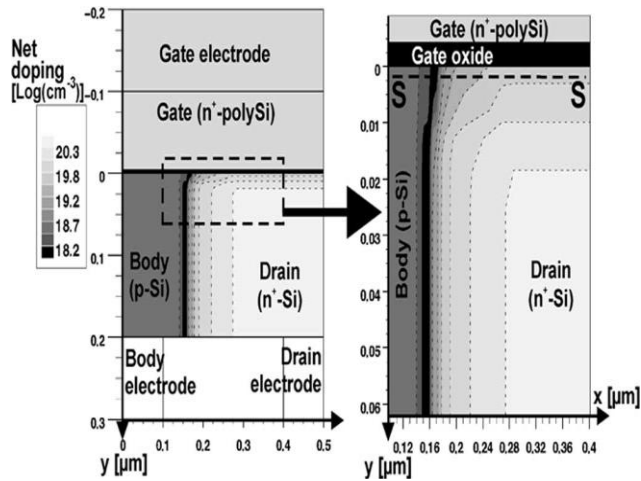


Fig. 2. Simulation of the GIDL with gated diodes [5]

The BTBT generation (hole–electron pairs) rate (GBBT) in gate-induced drain depletion regions is defined as in eq (1) where it changes with the total electric field in the region ($E_{TOT} = (E_x^2 + E_y^2)^{1/2}$).

$$G_{BBT} = AE_{TOT}^2 e^{-\frac{B}{E_{TOT}}} \quad (1)$$

Where $A = 9.66 \times 10^{18} / V^2 \cdot s^1 \cdot cm^1$, $B = 3 \times 10^{17} V/cm$. (Fig. 2).

GIDL current is characterized in [6] for 45-nm MOSFETs, where the GIDL current increases with increase in channel-doping levels. The GIDL as discussed in [6], is the result of electrons tunneling through reverse-biased junction (channel-to-drain pn). The measured GIDL is fitted using a BTBT model under different bias conditions and channel-doping levels. The modeled results were matched to experimental data to the full extent. To add, GIDL current dependency on lateral electric field, body bias, temperature and channel width is discussed and characterized [6]. Leakage currents were measured for on PMOS and NMOS devices (45nm low power). For accurate measurement of GIDL, polyfingers, in large number, are connected parallel. Different threshold voltages (V_{TH} of MOSFETs (low, medium, high) were studied. The variation (during the process step) in implantation dose resulted in different channel-doping levels thereby different V_{TH} (high for , medium and low for high, medium and low V_{TH} respectively).

The dependency of off-state GIDL on drain bias and gate length, with depleted SOI (fully) -channel (irradiated) MOSFETs, is presented in [7]. The observations were drawn from the experiments conducted, based on the model devised from the effects of the trapped charge in the oxide and of BBT. A systematic comparison of random telegraph noise in GIDL is presented in [8]. Both emission (τ_e) and capture (τ_c) times, depend on V_{GS} . However, τ_e has a strong dependency on temperature as τ_e decreases more than τ_c with temperature increase, and with increase in V_{GS} τ_c in the GIDL current increases.

RTN and gate Edge Direct Tunneling (EDT), were characterized in MOSFETs with high dielectric constant k , under GIDL bias conditions, [9]. It shows that, two independent traps produce four-level RTN, in the high- k gate dielectric. Further, the fundamental physics was provided in [9], to explore and analyze the leakages due to BTBT in MOSFETs at nano scale level.

A high- k gate dielectric nFET with HfSiON is used in [9] for experimental works, which is formed by high- k dielectric deposition, after chemical cleaning, using a deposition method called Atomic Layer Deposition (ALD). The 20% concentrated HfO₂ is deposited, and then nitrided and annealed with plasma nitridation. Then, using ALD, TiN electrodes were deposited, making stacked TiN gate electrode. HfSiON high- k layer, and a SiO₂ IL (with ~0.6 nm thickness), were laid with ALD. A well-controlled short-channel device fabricated using CMOS process with a lightly doped drain (rapid thermal annealing at 1000 °C, used for halo implantation) with CoSi₂, and a Ti/TiN/W. The transistors had gate with 10 μm and 0.06–0.5 μm of width and length respectively.

GIDL in FinFET devices are investigated through 3-D process in [10], with thick-oxide dual-gate channel without doping and with doping. It is studied in [10], that for a given gate dielectric thickness and gate length (L_G), the GIDL is effected tremendously by grading and placement of the drain junction and the channel doping. Further, it was argued in [10] that, with formation of steep underlapped junctions, GIDL can be suppressed by two orders of magnitude, for both undoped and doped channels.

The metal(TiN) layers and gate dielectric (SiO₂ and HfO₂) were deposited(The gate-first process was used for experimenting) after fin patterning. The fins were merged by $2 \times 10^{20} \text{ cm}^{-3}$ (source/drain)p-doped Si epitaxial, after defining gate and spacer. After implanting as vertically, a second spacer was then patterned at 12 keV, with a dosage of $2 \times 10^{15} \text{ cm}^{-3}$. The laserannealing done after dopant diffusion/activation using RTA at 1000 °C. Device model calibrations done using the experimental simulations in [10] on nFET devices with variation of LG (60 to 60 nm). Few investigations on RTN in GIDL current of aMOSFET are presented in [11], where, the capture cross section (σ_c) was extracted, introducing a more accurate σ_c by analyzing bias dependence of σ_c . pMOSFET, with Silicon-germanium (SiGe) channel, is considered to be an alternative for the conventional channel device (silicon only) for 32-nm above, due to its higher channel mobility and lower threshold voltage. For high threshold voltage and low leakage, designs, lower SiGe bandgap makes GIDL an important parameter. The GIDL and performance dependency on pre-halo/LDD Ge pre-amorphization implant (PAI) is investigated using experimental simulations in [12], where it is observed, that GIDL reduced by about ~40% without Ge PAI and achieved 50% reduction in total leakage (I_{OFF}) with PAI for similar processing. At the sidewall junction regions (source/drain), eliminating end-of-range defects, reduces GIDL, and improves I_{ON}/I_{OFF} ratio ([12]). Further, it was observed in [12] that, because of an increase (small) in the extrinsic resistance (series), I_{ON} experiences a small reduction without Ge PAI. The GIDL is statistically analysed in [12] for set of devices with similar geometry which are considered to be identical (nominally). A log-normal distribution behaviour of GIDL (the cumulative probability) ([12]) is presented Fig. 3(a), where the scale parameter is a function of drain bias (Fig 3(b)). It is evident from experiments in [12] that statistical dispersion is without PAI indicating trap-induced variability as the traps were distributed randomly.

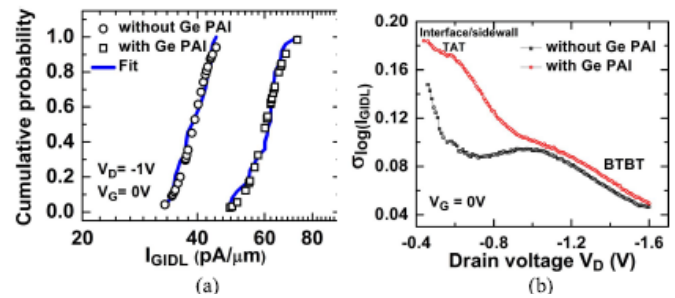


Fig. 3. (a) GIDL Cumulative probability ($V_D = -1\text{V}$), (b) GIDL statistical variation.

Physical features of GIDL in Silicon Nano Wire Transistors (SNWTs) (gate-all-around) are verified, with proper experimentations, in [13]. The results show that, under low $|V_{gs}|$, the SNWTs suffer from a severe GIDL with shrinking of device diameter (D_{nw}). With relatively large D_{nw} , and at high $|V_{gs}|$ the traditional transverse BTBT (T-BTBT) is dominant. The study of GIDL dependence on doping, overlap length (L_{ov}), and D_{nw} cross-sectional shape reveals that both the tunnelling methods (T-BTBT and L-BTBT) were improved by rounded corners with reduced doping. GIDL, for the Vertically Stacked Nano Wire (VS-NW) FETs, was comprehensively analyzed in [14]. The two modes (VS-NW), were compared, namely junctionless mode (JM) and inversion mode (IM). It was observed in [14], by numerical simulations, that the GIDL of IM-FET was larger than that of JM-FET. It was found ([14]) that the difference in drain/source (D/S) doping concentration creates difference between the IM and JM-FETs as depletion width becomes the tunnelling width. The experimental results ([14]) showed that longitudinal BTBT, significantly controls GIDL current of the NW FET rather than the transverse BTBT. The reduction of GIDL is reported in [15], for p-type polycrystalline-silicon thin-film transistor. The reduction was observed ([15]) due to trapping and local electron generation near kink current region, during the drain bias sweep. The reduction of the GIDL current during drain bias sweeps at successively lower gate biases undergoes a two-stage evolution behaviour. The

mechanism for leakage current (two-stage reductionbehaviour) is clarified with the comparison of the activation energy for the leakage currents after proper extraction before and after the drain bias sweeps. Moreover, drain bias sweeps improves the uniformity of the leakagecurrents effectively.

A comprehensive analysis of GIDL was performed in [16], in nanotube (NT) and nanowire (NW) of FETs. [16] Demonstratesincreasing currents in OFF-state with additionalL-BTBT. The performance of NTFETs significantlydegraded with increase in L-BTBT with the scaled gates to sub-10-nm. But, theperformance is improved though the core gate increases the gate capacitance of NTFETs [16]. Further, [16] provides the design guidelines for NTFETs such as dielectricconstant(spacer), t_{ox} (effective),NT diameter, intrinsic material bandgap and supplyvoltage (L-BTBT).

The formation of a BJT(parasitic)during the OFF-state ($V_{GS} = 0.0$ V) is discussed in [17], for nanowire FETs, due to LTBT of GIDL with details of the difference in GIDL nature, i.e., the negative gate voltage ($V_{GS} \leq 0$ V) effect on drain current fordifferentNWFET configurations. The significance of shown in parasitic BJT action was discussed in [17], in NW,JMFET and NW MOSFET inthe OFF-state which diminishes for the negative gate voltages. In addition, [17] proposed the use of anLDDE for increasing I_{ON}/I_{OFF} of NW MOSFET and NW JMFET.

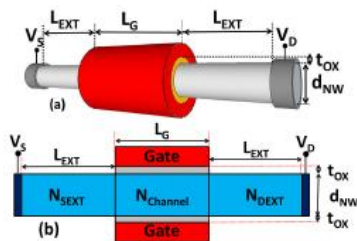


Fig. 4. NW FET. (a) 3-D view. (b) Cross-sectional view.

[17] Used Lombardi mobility, Philips unified mobility for simulating the 3D models in sentarus TCAD with Auger recombination model, Fermi–Dirac and Shockley–Read–Hall statistics. The corresponding results are tabulated in Table I.

TABLE I

Parameter	MOSFET	JLFET	JAMFET
Nanowire Diameter (d_{NW})	5 – 10 nm	5 – 10 nm	5 – 10 nm
Effective gate oxide thickness (EOT) (t_{ox})	1 nm	1 nm	1 nm
Source Extension doping (N_{SEXT})	$N_D = 1 \times 10^{20}$ cm ⁻³	$N_D = 1 \times 10^{19}$ cm ⁻³	$N_D = 1 \times 10^{20}$ cm ⁻³
Drain Extension doping (N_{DEXT})	$N_D = 1 \times 10^{20}$ cm ⁻³	$N_D = 1 \times 10^{19}$ cm ⁻³	$N_D = 1 \times 10^{20}$ cm ⁻³
Channel doping ($N_{Channel}$)	$N_A = 1 \times 10^{16}$ cm ⁻³	$N_D = 1 \times 10^{19}$ cm ⁻³	$N_D = 1 \times 10^{18}$ cm ⁻³
Gate work function	4.4 eV	4.8 eV	4.6 eV
Gate length (L_g)	5 – 20 nm	5 – 20 nm	5 – 20 nm
Length of Source/Drain extensions (L_{EXT})	25 nm	25 nm	25 nm

The GIDL increases in the gate, along with BTBT, Trap-Assisted Two-Step Tunnelling (TATT). The effect of interface traps generated was quantitatively analyzed in [18], that creates OFF state stress causing deterioration in GIDL.

TABLE II

Type of Transistor	Conventional with GPox 80Å		Conventional with GPox 60Å		DOI with GPox 60Å	
	Ion @ 2.0V	Ioff @ 2.2V	Ion @ 2.0V	Ioff @ 2.2V	Ion @ 2.0V	Ioff @ 2.2V
Peripheral NMOS	250 μ A/ μ m	0.8 pA/ μ m	280 μ A/ μ m	5 pA/ μ m	350 μ A/ μ m	4 pA/ μ m
Peripheral PMOS	95 μ A/ μ m	1 pA/ μ m	110 μ A/ μ m	6 pA/ μ m	130 μ A/ μ m	1 pA/ μ m
Pull-Down Transistor	35 μ A	100fA	45 μ A	100fA	45 μ A	100fA
Pass Transistor	30 μ A	80fA	40 μ A	80fA	40 μ A	80fA
Load Transistor	15 μ A	200fA	20 μ A	500fA	25 μ A	100fA

GIDLincreases with the applied stress, while device performance such as ON-state current(I_{ON})andtransconductance (gm) degrades due to interface traps simultaneously. By usingthe CP characterization, along the junction (gate-to-drain overlap region), the interface traps were spatially profiled. Further, inside energy band, trap distribution was alsocharacterized.

III. Applications And Architectures for GIDL

A technology called double offset-implanted (DOI) was proposed in [19], to suppress the GIDL in a PMOS transistorburied-channel. The DOI uses SiN etch-stopper scheme, in forming borderless W-contact offset spacer process. TheS/D to overlap can be made controllable by using DOI technology. Furthermore, CMOS transistorperformance can be enhanced by reducing the sidewall re-oxidationthickness and optimized implantation, to improve further the performance of each transistor, with operating voltage margin as low as possible andthe device speed lower than that of the

conventional at 80 Å. Table II depicts the leakage and the current transistor performance with DOI (compared against conventional approach). GIDL currents with Bulk trap enhanced (BTE) in high-κ MOSFETs are studied and reported in [20], along with the GIDL dependency on electrical stress, high-κ film thickness and the effect of Zr concentration in HfZrO_x. Adding Zr into HfO₂ reduces GIDL with high-κ film (thinner).

It was successfully demonstrated GIDL improvements, on a DRAM product, by Millisecond Flash anneal (MFLA) ([21]). MLFA proved to be potential for DRAM application based on the fundamental studies made on the device characteristics such as blanket wafers and product wafers. The reduction of about 36% is observed in periphery NMOS off current in [21] with the conductor devices demands, minimize phenomena of myriad leakage with a very good ability to quantitatively model. A model (physical) is proposed in [22] to quantitatively explain the GIDL dependency on orientation, which is a very important in next-generation design of silicon based devices at nano scale. The appropriate choice of doping, materials, device geometries and process conditions to alleviate the problem of GIDL can be predicted using the model in [22].

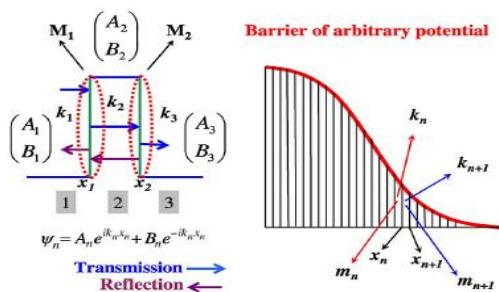


Fig. 5. Importance of Transfer matrix method.

In GIDL, the tunneling of electron from drain conduction band to substrate valence band is used to model BTBT. Fig. 6 shows portion of the junction region with BTBT [22] (zoomed in). The transfer matrix, as shown in Fig. 6, ([22]) has the similarity with the wavefunction in the regions of substrate and drain. The n^{th} interface transfer matrix is

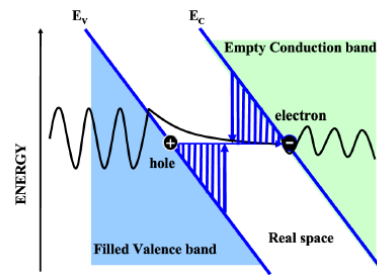


Fig. 6. Schematic diagram of tunneling from valence band to conduction band

$$M_n = \frac{1}{2k_n m_{n+1}} \begin{bmatrix} C e^{i(k_{n+1}-k_n)x_n} & D e^{-i(k_{n+1}+k_n)x_n} \\ D e^{i(k_{n+1}+k_n)x_n} & C e^{i(k_{n+1}-k_n)x_n} \end{bmatrix} \quad (2)$$

with $C = (k_n m_{n+1} + k_{n+1} m_n)$ and $D = (k_n m_{n+1} - k_{n+1} m_n)$, $k_n(k_{n+1})$ -wave vector and $m_n(m_{n+1})$ - e^- effective mass left (right)- of the n^{th} interface. $x_n(x_{n+1})$ - distance of the n^{th} ($(n+1)^{\text{th}}$) interface, as depicted in Fig. 5. The wavefunction of the incoming and outgoing electron related to each other as

$$\begin{bmatrix} A_1 \\ B_1 \end{bmatrix} = [M_1 \otimes M_2 \otimes \dots \otimes M_n \otimes M_{n+1}] \begin{bmatrix} A_{n+2} \\ B_{n+2} \end{bmatrix} \quad (3)$$

where A_n -forward and B_n - backward-propagating wavevectors, respectively. The transmission coefficient is defined as

$$T(E) = \left| \frac{A_{n+2}}{A_1} \right|^2 \quad (4)$$

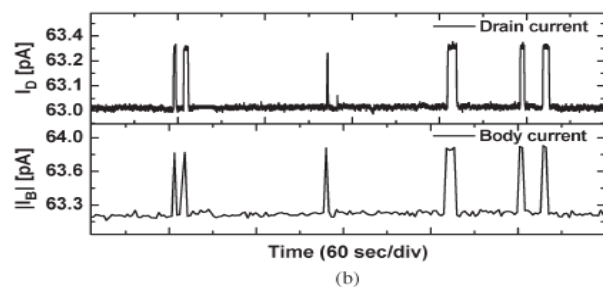
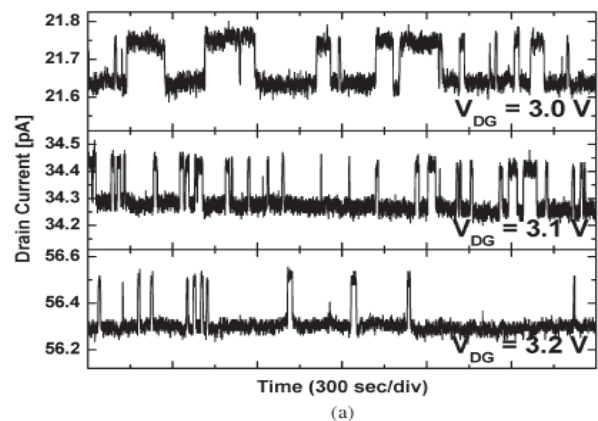


Fig. 7. IGIDL RTN (a) Change of IGIDL RTN with V_{DG} . (b) RTN.

The tunneling current using transmission coefficient is written as

$$dJ_{tun} = \frac{em * k_B T}{2\pi^2 \hbar^3} T(E_x) \ln \left[\frac{1 + \exp\left(-\frac{E_x - E_{FP}}{k_B T}\right)}{1 + \exp\left(-\frac{E_x - E_{FN}}{k_B T}\right)} \right] dE_x \quad (5)$$

GIDL simulation results are (The 45-nm n-MOSFET) for presenting more complex structures (for device) and future nodest in view of modeling GIDL effectively. In general, this method, with BTB tunneling as dominant form of tunneling, is applicable to any type of transistors. The simulations on MOSFETs clarifies why the [100] on vertical diodes with preferably n-orientation to minimize GIDL currents.

An accurate method is developed in [23] for extracting the energy level and depth of an oxide trap from RTN in the GIDL current of a MOSFET) that employs trap capture and emission times.

The absolute and relative amplitudes of I_{GIDL} RTN, ΔI_{GIDL} and $\Delta I_{GIDL}/I_{GIDL}$ respectively, are defined (due to a captured electron in the oxide trap at the overlap region) as

$$\frac{\Delta I_{GIDL}}{I_{GIDL}} = \frac{I_{GIDL}(F + \Delta F) - I_{GIDL}(F)}{I_{GIDL}(F)} \quad (7)$$

where F - electric field, and ΔF - increment of the electric field. RTN amplitude for the reference current to normalize is the low level current with empty trap. The changes in amplitudes of RTN with respect to V_{DG} are estimated. The I_{GIDL} is expressed as shown in eq. (8),

$$I_{GIDL} = S \frac{A}{B} F^\sigma \exp\left(-\frac{B}{F}\right) \quad (8)$$

If $\Delta F \ll F$, ΔI_{GIDL} and $\Delta I_{GIDL}/I_{GIDL}$ can be written as follows: by substituting the expansion of (8) in (7) and (6)

$$\frac{\Delta I_{GIDL}}{I_{GIDL}} \approx \frac{I_{GIDL}(F) \left[\exp\left(\frac{B}{F^2} \Delta F\right) - 1 \right]}{I_{GIDL}(F)} \quad (9)$$

Further, it is evident from [23], at 32-nm node (for pMOSFETs), and beyond, Silicon-germanium

combination is considered to be an alternative channel because of its higher carrier mobility in the channel of high-k metalgate and lower threshold technology. However, because of BTB and TAT, at low power technology nodes, GIDL is becoming a major concern, due to bandgap reduction.

The GIDL dependence on drain and substrate bias as well as temperature is presented in [24]. The GIDL during off state, near the drain surface, is mostly due to the phonon-assisted BTBT in the top SiGe layer and at the drain sidewall junction (from TCAD simulations in [24]). It is observed in [25] that TAT at the extension/sidewall is dominant for other substrate bias, gate and drain voltages.

In [25], an ultrathin channel of poly-Si transistors (thin-film), is proposed, with Q-LDD structure and considerable reduction in kink current. The doping concentration was adjusted, on the poly-Si channel, by varying the thickness in LDD and drain-source region. The Q-LDD proposed in [25], showcases the advantages of a thin channel and a thin-gate insulator, in contrast to the thick oxide conventional sidewalls. The GIDL currents were suppressed successfully without sacrificing ON-current and threshold voltage. The GIDL characteristics in a gated-diode memory cells (as a cell string) are presented in [26], with a gate dielectric stack of oxide-nitride-oxide (O/N/O) for gate diodes, for implementing a non-volatile type of memory with a select MOSFET and investigated the performance of memory. 1×6 cell string is used to demonstrate a 6-b digital to analog converter (DAC) with binary-weighted current-steering.

The impact of the design of gate sidewall spacer was studied for the first time in [27], on the GIDL of NWFETs for a gate-S/D (underlap) extension and the traditional nanowire (NW) FETs. Suppressed L-BTBT is resulted from the inclusion of a high-k spacer over the S/D extension in the traditional/conventional NWFETs. An analysis was presented in [28] for hetero-dielectric with dual-metal (DM-HD) GAAMOSFET to solve a substantial issue of GIDL current in quest of

improving the device reliability, BTBT and leakages, by reducing OFF-state leakages due to tunnelling width enhancement and source to channel barrier height increment. It is observed from [28] that OFF-state leakage in DM-HDGAA MOSFET reduced from 10^{-9} to an order of 10^{-130} A. OFF-state leakages have been analysed at higher temperatures.

Direct estimation of the phonon energy is presented in [29] (hot carriers) by measuring GIDL. Gate oxide aging was cured by GIDL current, in a GAA FET which is fabricated on a substrate (bulk) ([30]). During the off-state, hot-carrier injection (HCI) leads to large GIDL there by curing the aging of gate oxide with the elevated temperature. GAAFETs on a p-type (100) bulk Si-wafer ([31]) was fabricated using reactive ion etching process. First, HCI stress intentionally applied to accelerate aging by gate voltage (V_G) of 3 V and a drain voltage (V_D) of 6 V for the duration of 200 s then, curing voltage applied to increase I_{GIDL} . Sub-threshold swing (SS) threshold voltage (V_{TH}) and) were extracted after curing the GAA FET at $V_G = -4$ V with an I_{GIDL} of 50 μ A and $V_D = 4.05$ V for 50 ms.

IV. Analysis and Modelling Of GIDL

GIDL strongly dependent on temperature, due to TAT, based on the Shockley–Read–Hall (SRH) equation. The model in [32], successfully reproduced the results with experiments. P-MOSFET temperature dependency calculated with single fitting parameter, (interface trap density for $= 1 \times 10^{14}$ (1/eV m^2)).

A GIDL model was presented in [33] to avoid the 1-D models invalidation for FDDG MOSFETs by solving 2-D Poisson equation and tunneling theory systematically. The following equations (11) TO (16) depict the flow.

The tunneling probability T_t presented in (11) (Wentzel–Kramers–Brillouin method)

$$T_t = \exp\left(-\frac{\pi m^{*1/2} E_g^{3/2}}{2\sqrt{2}q\hbar\xi}\right) \quad (11)$$

Where, E_g - energy gap, ξ - field intensity, and m^* - effective mass. The total energy E is divided as E_{\parallel} and E_{\perp} , (parallel to tunneling and transverse energy normal to tunneling). The tunneling probability with E_{\perp} is

$$T_t = \exp\left(-\frac{\pi m^{*1/2} E_g^{3/2}}{2\sqrt{2}q\hbar\xi}\right) \exp\left(-\frac{2E_{\perp}}{\bar{E}}\right) \quad (12)$$

where \bar{E} ,

$$\bar{E} = \frac{4\sqrt{2}q\hbar\xi}{3\pi m^{*1/2} E_g^{1/2}} \quad (13)$$

The incident flux (/ unit volume / second) is

$$F = \frac{q^2 m^* \xi}{2\pi^2 \hbar^3} f(E) dE_{\perp} \quad (14)$$

The the tunneling current is as shown in (15)

$$I_t = \int T_t F dV = \int_0^W dz \int_0^{L_{ov}} dy \int_0^a dx \int_0^{\infty} dE_{\perp} \times \frac{q^2 m^* \xi(x, y) [(1 - f(E_v)) - f(E_c)]}{2\pi^2 \hbar^3} T_t \quad (15)$$

Here, $f(E_v)$ and $f(E_c)$ - Fermi–Dirac distributions (in the valence band and electron in the conduction band).

The integration in (15) about E_{\perp} and z is first evaluated and simplified as in (16)

$$I_t = 2 \int_0^{L_{ov}} dy \int_0^a dx \frac{\sqrt{2} q^3 m^{*1/2} W |\xi(x, y)|^2}{3\pi^2 \hbar^2 E_g^{1/2}} \times \exp\left(-\frac{\pi m^{*1/2} E_g^{3/2}}{2\sqrt{2}q\hbar|\xi(x, y)|}\right) \quad (16)$$

In unified RAM (URAM), A soft-programming-free operation is presented in [34] where, to provide the versatile functions 1T-DRAM, as well as nonvolatile memory, with mode selection according to the designer's demand, a floating-body and an O/N/O layer were integrated into FinFET [(34)],

Undesired O/N/O softcharge trapping changes threshold voltage gradually, making URAM unstable. GIDL program method is proposed in [34] to avoid the threshold shift in soft programming and improve immunity to disturbances.

The dependency of GIDL on the back-gate bias, with ultrathin body (UTB) silicon-on-insulator (SOI) modelling of MOSFETs were presented in [35], and also presents the model for gate bias-dependent gate current with proven analysis. Popular compact model

with industry standard, BerkeleyShort-channel IGFET Model- uses GIDL dependency on these back bias- and gate current with good correlation to experimental data.

Strong dependency of GIDL on drain voltage at off state is explore in [36]. An inversion layer is formed, because of highD-G voltage ($V_{DG} = V_{DS} - V_{GS}$), in source drain overlap leading to BTBT, modelled in [36].

$$I_{GIDL} = AGIDL \cdot W \cdot E^{PGIDL} \cdot \exp\left(-\frac{BGIDL}{E}\right) \quad (17)$$

where W - width, E - electric field in the overlapregion and AGIDL, PGIDL, and BGIDL- the model parameters. E can be expressed as in (18).

$$E = \frac{V_{DS} - V_{GS} + V_{FBSD} - EGIDL}{\epsilon_{ratio} EOT1} \quad (18)$$

Here,EGIDL - model parameter V_{DS} - drain voltage,, V_{FBSD} flat band voltage and V_{GS} -front gate voltage, EOT1 -effective front gate oxide thickness, ϵ_{ratio} - semiconductor to front gateoxide permittivity ratio.

The effects ofback-gate bias (Fig 8) is the shift in threshold voltage (By Gauss's law)

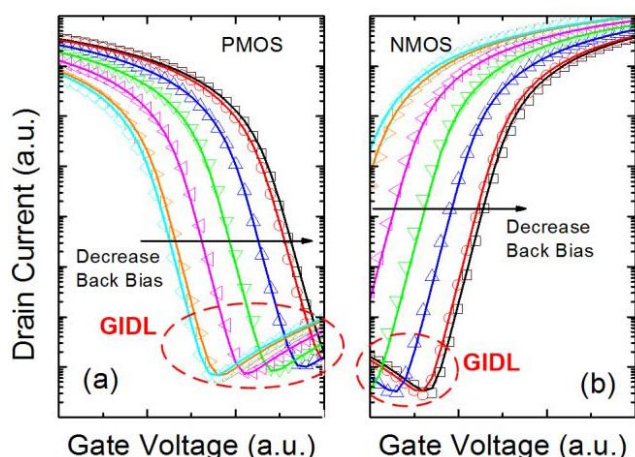


Fig. 8. UTB SOI ID–VG characteristics (a) P-MOSFET and(b) N-MOSFET.

in the overlap region, making V_{GS} in eq.(18) an effective front gate voltage $V_{GS\text{eff}}$ in eq.(19)

$$V_{GS\text{eff}} = V_{GS} - VBGLDL \cdot \gamma_0 \cdot (V_{BGS} - V_{FBSDBG} - VBEGIDL) \quad (19)$$

where, V_{FBSDBG} -flat band voltage, $VBEGIDL$ and $VBGLDL$ - the model parameters in the overlap

region, and γ_0 is the capacitive coupling between the body and the back- [37], [38].

$$\gamma_0 = -\frac{C_{Si} \cdot C_{OX2}}{(C_{Si} + C_{OX2}) \cdot C_{OX1}} \quad (20)$$

where C_{Si} -thinbody, C_{OX2} -back gate, and C_{OX1} -front gatecapacitances respectively. $VBGLDL$ is around 1, while $VBEGIDL$ is about 100 mV. In (20), the body is assumed to be fully depleted is C_{Si} is a constant ($=\epsilon_{Si}/T_{Si}$). The effective front gate voltage is effected by the back-gate bias forMOSFET (eq. (18,19,20)). Thismodel is implemented into BSIM-IMG, with a good correlation of experimentation (as presented Fig.8).

An analysis is proposed in [39] where, 2-D Poisson's equations were used in modelling electricfield E_z , Surface potential, and I_{GIDL} , with appropriate boundary conditions. In [39], the DIBL phenomenon and electronvelocitythe effect oftemperature on gm, gd, noise figure, and noise conductance were tested experimentally.

$$I_{GIDL} = AE_i^2 \left(\frac{t_{si}}{2}, L_1 + L_2\right) \exp\left(\frac{-B}{E_i \left(\frac{t_{si}}{2}, L_1 + L_2\right)}\right) \quad (21)$$

where A and B are the constants [40]: $A = \frac{q^2 m_r^{1/2}}{18\pi \hbar^2 E_{gap}^{1/2}}$ and $B = \frac{\pi m_r^{1/2} E_{gap}^{1/2}}{2\sqrt{2} q \hbar} = 21.3 \text{ MV/cm}$.

$q - e^-$ charge, $m_r = 0.2 m_0$, E_{gap} - direct energy gap of silicon and \hbar - Planck constant.

I_{sub} is the current for $0 \leq V_{gs} \leq V_{th}$ (subthreshold region). [41] modelled temperature-dependent GIDL in FinFETs. BTBT only is used to model GIDL mechanism in BSIM-CMGfor FinFET, which is insufficient in capturing the GIDL at low electric fields. TAT was captured at low electricfields and BTBT was at a high fields as presented in [41], with a single piece wise expression for TAT GIDL current, present in the FinFET node at sub-20-nm technology. GIDL current is expressed as shown in eq [22], by integrating generationrate of electron/hole pair [42].

$$I_{GIDL} = I_{BTBT-GIDL} + I_{TAT-GIDL} = W \cdot q \iint (G_{BTBT} + G_{TAT}) dx \cdot dy \quad (22)$$

Finally, including V_{db} dependency (22) can be expressed as follows

$$I_{GIDL} = (I_{BTBT-GIDL} + I_{TAT-GIDL}) \cdot \frac{V_{db}^2}{CGIDL + V_{db}^2} \quad (23)$$

where CGIDL - model parameter [43], [44].

Further, the effect of Lun (drain-gate underlap), on an LNA (narrow band) performance has been studied, [45]. SOI-based and bulk-based junctionless FinFETs with heavy-ion irradiation are analysed with 3D-TCAD in [46]. The radiation performance of the planar junctionless devices (JLD) and the SRAMs using JLDs were analysed in [47]. The radiation tolerance of single ended and differential ring VCO was analysed in [48] in the presence of SET using 90 nm CMOS technology.

V. Conclusion

Major leakage at gate-drain overlap region is the Gate-Induced Drain Leakage (GIDL) which is becoming one of the important performance metric in current low power and submicron technologies. Dynamic Random Access Memories (DRAM's) are the most effected systems due to GIDL current, as it is the major source of leakage of a transistor. The retention time degradation in DRAM's is greatly influenced by OFF-STATE leakage in MOSFETs. In this article, the effect of different parameters like minimize short-channel effects, including subthreshold leakage, while maximizing transconductance and saturation current have been studied.

References

- [1] Siguang et. al, " Gate-Induced Drain Leakage Current Enhanced by Plasma Charging Damage", Electron Devices IEEE Transactions On, , MAY 2001, Vol. 48, No. 5, pp-1006-1008.
- [2] S.Mahapatra, et. al, "A comprehensive study of hot-carrier induced interface and oxide trap distributions in MOSFETs using a novel charge pumping technique," Electron Devices, IEEE Trans On., vol. 47, Jan. 2000, pp. 171–177,
- [3] Ja-Hao Chen, et. al, , "DC Pulse Hot-Carrier-Stress Effects on Gate-Induced Drain Leakage Current in n-Channel MOSFETs", Electron Devices, IEEE Trans, December 2001 Vol. 48, No. 12,
- [4] Oleg Semenov et. al, "Impact of Gate Induced Drain Leakage on Overall Leakage of Submicrometer CMOS VLSI Circuits", Semiconductor Manufacturing, IEEE Transactions On, February 2002. Vol. 15, No. 1,
- [5] Enrico Gili et. al, "Asymmetric Gate-Induced Drain Leakage and Body Leakage in Vertical MOSFETs With Reduced Parasitic Capacitance", Electron Devices, IEEE Trans On, May 2006, Vol. 53, No. 5,
- [6] Xiaobin Yuan et. al, "Gate-Induced-Drain-Leakage Current in 45-nm CMOS Technology", Device And Materials Reliability, IEEE Transactions On, September 2008. Vol. 8, No. 3,
- [7] Farah E. Mamouni et. al, "Gate-Length and Drain-Bias Dependence of Band-to-Band Tunneling-Induced Drain Leakage in Irradiated Fully Depleted SOI Devices", Nuclear Science , IEEE Transactions On, December 2008, Vol. 55, No. 6..
- [8] Ju-Wan Lee et. al, "Comparison of Low-Frequency Noise in Channel and Gate-Induced Drain Leakage Currents of High-k nFETs", Electron Device Letters, IEEE, Vol. 31, No. 10, October 2010
- [9] Ju-Wan Lee et. al, "Investigation of Random Telegraph Noise in Gate-Induced Drain Leakage and Gate Edge Direct Tunneling Currents of High-k MOSFETs", Electron Devices, IEEE Transactions On, April 2010, Vol. 57, No. 4.
- [10] Pranita Kerber et. al, "GIDL in Doped and Undoped FinFET Devices for Low-Leakage Applications", Electron Device , IEEE Letters, Vol. 34, No. 1, January 2013
- [11] Sung-Won Yoo et. al, "Capture Cross Section of Traps Causing Random Telegraph Noise in Gate-Induced Drain Leakage Current", Electron Devices, IEEE Transactions On, Vol. 60, No. 3, March 2013
- [12] Vishal A. Tiwari et. al, "Effect of Germanium Pre-amorphization Implant on Performance and

- Gate-Induced Drain Leakage in SiGe Channel pFET”, *Electron Device*, IEEE Letters, Vol. 36, No. 6, June 2015.
- [13] Jiewen Fan et. al, “Insight Into Gate-Induced Drain Leakage in Silicon Nanowire Transistors”, *Electron Devices*, IEEE Transactions On, Vol. 62, No. 1, January 2015
- [14] Jae Hur et. al, “Comprehensive Analysis of Gate-Induced Drain Leakage in Vertically Stacked Nanowire FETs: Inversion-Mode Versus Junctionless Mode”, *Electron Device*, IEEE Letters, Vol. 37, No. 5, May 2016.
- [15] Dongli Zhang et. al, “Investigations on the Gate-Induced Drain Leakage Current of Polycrystalline-Silicon Thin-Film Transistor and Its Suppression With Drain Bias Sweep”, *Electron Devices*, IEEE Transactions On, Vol. 63, No. 4, April 2016.
- [16] Shubham Sahay et. al, “Comprehensive Analysis of Gate-Induced Drain Leakage in Emerging FET Architectures: Nanotube FETs Versus Nanowire FETs”, IEEE Access, 2017, Digital Object Identifier 10.1109/ACCESS.2017.2751518.
- [17] Shubham Sahay et. al, “Physical Insights Into the Nature of Gate-Induced Drain Leakage in Ultrashort Channel Nanowire FETs”, *Electron Devices*, IEEE Transactions On Vol. 64, No. 6, June 2017.
- [18] Geon-Beom et. al, “Effect of OFF-State Stress on Gate-Induced Drain Leakage by Interface Traps in Buried-Gate FETs”, *Electron Devices*, IEEE Transactions On, Vol. 66, No. 12, December 2019
- [19] Sang-Hun Seo, et. al, “A Novel Double Offset-Implanted Source/Drain Technology for Reduction of Gate-Induced Drain Leakage With 0.12- μ m Single-Gate Low-Power SRAM Device”, *Electron Device*, IEEE Letters, Vol. 23, No. 12, December 2002.
- [20] J. C. Liao et. al, “Investigation of Bulk Traps Enhanced Gate-Induced Leakage Current in Hf-Based MOSFETs”, *Electron Device* IEEE Letters, Vol. 29, No. 5, May 2008.
- [21] Shian-Jyh Lin et. al, “Gate-Induced Drain Leakage (GIDL) Improvement for Millisecond Flash Anneal (MFLA) in DRAM Application”, *Electron Devices*, IEEE Transactions On, Vol. 56, No. 8, August 2009.
- [22] Rajan K. Pandey et. al, “Crystallographic-Oriented-Dependent Gate-Induced Drain Leakage in Nanoscale MOSFETs”, IEEE Transactions On, Vol. 57, No. 9, September 2010
- [23] Byoungchan Oh et. al, “Characterization of an Oxide Trap Leading to Random Telegraph Noise in Gate-Induced Drain Leakage Current of DRAM Cell Transistors”, *Electron Devices*, IEEE Transactions On, Vol. 58, No. 6, June 2011
- [24] Vishal A. Tiwari et. al, “Analysis of Gate-Induced Drain Leakage Mechanisms in Silicon-Germanium Channel pFET”, *Electron Devices*, IEEE Transactions On, Vol. 61, No. 5, May 2014.
- [25] Jae Hyo Park et. al, “A Novel Design of Quasi-Lightly Doped Drain Poly-Si Thin-Film Transistors for Suppression of Kink and Gate-Induced Drain Leakage Current”, *Electron Device*, IEEE Letters, Vol. 36, No. 4, April 2015.
- [26] Chul-Heung Kim et. al, “GIDL Characteristics in Gated-Diode Memory String and Its Application to Current-Steering Digital-to-Analog Conversion”,
- [27] Shubham Sahay et. al, “Spacer Design Guidelines for Nanowire FETs From Gate-Induced Drain Leakage Perspective”, *Electron Devices*, IEEE Transactions On, Vol. 64, No. 7, July 2017
- [28] Sonam Rewari et. al, “Gate-Induced Drain Leakage Reduction in Cylindrical Dual-Metal Hetero-Dielectric Gate All Around MOSFET”, *Electron Devices*, IEEE Transactions On, Vol. 65, No. 1, January 2018.
- [29] Nak Won Yoo et. al, “Detection of Hot Carrier Generated Phonon Using the Gate-Induced Drain Leakage in the Silicon Chip”, *Electron Devices*, IEEE Transactions On, Vol. 65, No. 9, September 2018
- [30] Jun-Young et al, “Curing of Hot-Carrier Induced Damage by Gate-Induced Drain Leakage Current in Gate-All-Around FETs”, DOI 10.1109/LED.2019.2946393, IEEE Electron Device Letters.
- [31] D.-I. Moon et. al, “Silicon Nanowire All-Around Gate MOSFETs Built on a Bulk Substrate by All Plasma-Etching Routes,”

- IEEE Electron Device Lett.*, vol. 32, no. 4, pp. 452–454, Apr. 2011. doi: 10.1109/LED.2011.2106758.
- [32] Markus Rosar et. al, “A New Model for the Description of Gate Voltage and Temperature Dependence of Gate Induced Drain Leakage (GIDL) in the Low Electric Field Region”, *Electron Devices*, IEEE Transactions On, Vol. 47, No. 1, January 2000.
- [33] Xiaoshi Jin et. al, “A Gate-Induced Drain-Leakage Current Model for Fully Depleted Double-Gate MOSFETs”, *IEEE Trans On Elect Devices*, Vol. 55, No. 10, October 2008.
- [34] Jin-Woo Han et. al, “Gate-Induced Drain-Leakage (GIDL) Programming Method for Soft-Programming-Free Operation in Unified RAM (URAM)”, *IEEE Elect Dev Lett*, Vol. 30, No. 2, February 2009.
- [35] Yen-Kai Lin et. al, “Modeling of Back-Gate Effects on Gate-Induced Drain Leakage and Gate Currents in UTB SOI MOSFETs”, *IEEE Trans On Elect Devices*, VOL. 64, NO. 10, OCT 2017.
- [36] J. Chen, et. al, “Subbreakdown drain leakage current in MOSFET,” *IEEE Electron Device Lett.*, vol. 8, no. 11, pp. 515–517, Nov. 1987.
- [17] *BSIM-IMG102.7.0 Technical Manual*. [Online]. Available: <http://bsim.berkeley.edu/models/bsimimg/>
- [38] P. Kushwaha et al., “Modeling the impact of substrate depletion in FDSOI MOSFETs,” *Solid-State Electron.*, vol. 104, pp. 6–11, Feb. 2015.
- [39] Anubha Goel et. al, “Temperature-Dependent Gate-Induced Drain Leakages Assessment of Dual-Metal Nanowire Field-Effect Transistor—Analytical Model”, *IEEE Trans On Elect Dev*, Vol. 66, No. 5, May 2019.
- [40] S. Rewari et. al, “Gate-induced drain leakage reduction in cylindrical dual-metal heterodielectric gate all around MOSFET,” *IEEE Trans. Electron Devices*, vol. 65, no. 1, pp. 3–10, Jan. 2018.
- [41] Chetan Kumar Dabhi et. al, “Compact Modeling of Temperature-Dependent Gate-Induced Drain Leakage Including Low-Field Effects”, *IEEE Trans On ElecDev*, Vol. 66, No. 7, July 2019.
- [42] G. A. M. Hurkx, D. B. M. Klaassen, and M. P. G. Knuvers, “A new recombination model for device simulation including tunneling,” *IEEE Trans. Electron Devices*,
- [43] S. Khandelwal. (2015). *BSIM-CMG 110.0.0 Technical Manual*. [Online]. Available: <http://bsim.berkeley.edu/models/bsimcmg/>
- [44] Y. S. Chauhan et al., *FinFET Modeling for IC Simulation and Design: Using the BSIM-CMG Standard*. New York, NY, USA: Academic, 2015.
- [45] K.K. Nagarajan, Vinodhkumar and R. Srinivasan “Optimization of Gate–Source/Drain Underlap on 30 nm Gate Length FinFET Based LNA Using TCAD Simulations”, *WSEAS TRANSACTIONS on CIRCUITS and SYSTEMS*, Issue 11, Volume 11, November 2012.
- [46] N. Vinodhkumar, R. Srinivasan, “Heavy-ion irradiation study in SOI-based and bulk-based junctionless FinFETs using 3D-TCAD simulation” *Microelectronics Reliability* 55 (2015) 2647–2653.
- [47] N. Vinodhkumar, R. Srinivasan, “Radiation performance of planar junctionless devices and junctionless SRAMs”, *J Comput Electron* (2016) 15:61–66 DOI 10.1007/s10825-015-0748-3.
- [49] Maran Ponnambalam, N. Vinodhkumar, R. Srinivasan, Premanand Venkatesh Chandramani, “Phase displacement study in MOSFET based ring VCOs due to heavy-ion irradiation using 3D-TCAD and circuit simulation”, *Microelectronics Reliability* 65 (2016) 27–34.
- [47] N. Vinodhkumar, R. Srinivasan, “SET and SEU performance of single, double, triple and quadruple-gate junctionless FETs using numerical simulations” *Microelectronics Journal* 67 (2017) 38–42

Author Biographies:

B. Balaji Naik, has completed B. E. degree in Electronics and Communication Engineering in 2004 from GITAM College of Engineering and M. Tech. degree in VLSI

design and Embedded Systems in 2008 from the National Institute of Technology Rourkela. He is currently pursuing his Ph.D. He is currently working as Assistant Professor in EECE, School of technology, GITAM (Deemed to be University), Hyderabad. His research interest lies in Low Power VLSI Design and Hardware Security.



Srinivasa Rao Thamanam, has completed B. E. degree in Electronics and Communication Engineering in 2003 from Andhra University, and M. Tech. degree in Digital Systems in 2005 from the College of Engineering, Pune.

He is currently pursuing his Ph.D from JNTU Kakinada in Signal and Image Processing and working as Assistant Professor in EECE, School of technology, GITAM (Deemed to be University), Hyderabad. His research interest lies in Digital Image Processing, Low Power VLSI Design.



Dr Srinivas Sabbavarapu, has completed B. Tech. degree in Electronics and Communication Engineering in 2004 from V R Siddhartha Engineering College and M. Tech. degree in VLSI design

and Embedded Systems in 2008 from the National Institute of Technology Rourkela. He received his

Ph.D. from the Indian Institute of Technology (IIT), Hyderabad, India. He is currently working as Associate Professor in ANITS (Autonomous) Engineering College, Visakhapatnam. His research interest lies in CAD for VLSI, Low Power VLSI Design and Hardware Security.



K. Manjunathachari, has Ph.D from JNT University, Kakinada, and M.Tech from JNT University, Hyderabad, has an experience of more than 17 years of

Teaching and 3 years of Industry. At present Dr. K. Manjunathachari working with the GITAM University, Hyderabad, Telangana, as a Professor and Head of the EECE department. He published many papers in his field of interest viz. Signal and Image Processing.